

# Compounds from *Toddalia asiatica*: Immunosuppressant Activity and Absolute Configurations

Jakob K. Reinhardt, Amy M. Zimmermann-Klemd, Ombeline Danton, Martin Smieško, Carsten Gründemann, and Matthias Hamburger\*



Cite This: <https://dx.doi.org/10.1021/acs.jnatprod.0c00564>



Read Online

ACCESS |



Metrics & More

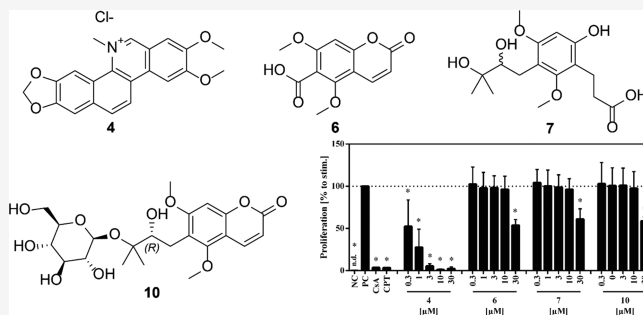


Article Recommendations



Supporting Information

**ABSTRACT:** In a screening of an extract library from plants used in Traditional Chinese Medicine the MeOH extract of *Toddalia asiatica* inhibited proliferation of human primary T cells with an  $IC_{50}$  of 25.8  $\mu\text{g}/\text{mL}$ . Activity in the extract was tracked by HPLC activity profiling, and a total of 15 compounds were characterized. Three compounds, toddalic acid (6) and both enantiomers (7a and 7b) of toddanolic acid (7), were new natural products, and two recently published compounds, (2'R)-toddalolactone 3'-O- $\beta$ -D-glucopyranoside (10) and (2'S)-toddalolactone 2'-O- $\beta$ -D-glucopyranoside (11), were described in detail for the first time. The absolute configurations of compounds 8, 9, 10, 12, 13, and 15 were determined by comparison of experimental and calculated ECD spectra. For glucosides 9 and 10, ECD data and chiral-phase HPLC of the aglycones after enzymatic hydrolysis confirmed the results. Nitidine chloride (4) inhibited proliferation of primary human T cells with an  $IC_{50}$  of 0.4  $\mu\text{M}$ .



Under normal conditions the immune system is able to differentiate between self and nonself.<sup>1</sup> However, autoimmune diseases can develop if this function is impaired. In rheumatoid arthritis, for example, autoreactive T cells attack the synovial lining of the joints, resulting in tissue destruction and inflammation.<sup>2</sup> Autoimmune diseases are typically treated with immunosuppressive drugs, but therapy may be accompanied by severe side effects.<sup>3</sup> Thus, there is a need for better-tolerated treatment options. To find new natural product leads with immunosuppressive activity, a library of extracts from plants used in Traditional Chinese Medicine (TCM) was screened for their ability to inhibit T cell proliferation in vitro. The MeOH extract from roots of *Toddalia asiatica* Lam. (Rutaceae) was a promising hit, as it showed an  $IC_{50}$  value of 25.8  $\mu\text{g}/\text{mL}$  without concomitant cytotoxicity (Figure S1, Supporting Information). *T. asiatica* grows in most parts of Asia and Africa.<sup>4</sup> Its roots are only occasionally used in TCM (Fei Long Zhang Xue),<sup>5</sup> but more commonly as an antimalarial drug in different African countries.<sup>6,7</sup> The phytochemistry of *T. asiatica* has been widely studied, and numerous coumarins, alkaloids, and phenolic compounds have been isolated from the roots of the plant.<sup>8–10</sup> Most notably, a structurally diverse set of coumarins have been identified, including glucosides and prenylated derivatives.

## RESULTS AND DISCUSSION

The active compounds in the extract were tracked by HPLC-based activity profiling.<sup>11</sup> The overlay of an analytical HPLC

chromatogram and the activity of 1 min microfractions collected is shown in Figure S2 (Supporting Information). Inhibition of T cell proliferation was found in the microfractions eluted at 14, 15, and 26 min. Compounds 3–10 in the time windows of activity were subsequently isolated by a combination of liquid–liquid partitioning, centrifugal counter-current chromatography, preparative flash chromatography, and HPLC on RP stationary phases. In addition, compounds 1, 2, and 11–15 were isolated from adjacent regions in the HPLC chromatogram (Figure S2, Supporting Information). The active fraction at 26 min contained a minor peak with the same mass as nitidine (4). However, this peak was not found after further fractionation of the extract.

Compound 1 was identified as syringic acid by analysis of HRESIMS and NMR data (Table S1, Supporting Information) and comparison with literature data.<sup>12</sup>

Compound 2 had a molecular formula of  $C_{21}H_{23}NO_5$  (HRESIMS data  $m/z$  370.1646  $[M + H]^+$ , calcd for  $C_{21}H_{24}NO_5^+$ , 370.1649). With the aid of 1D and 2D NMR data recorded at 23 and 60  $^{\circ}\text{C}$  (Table S2) and comparison

Received: May 22, 2020

Chart 1

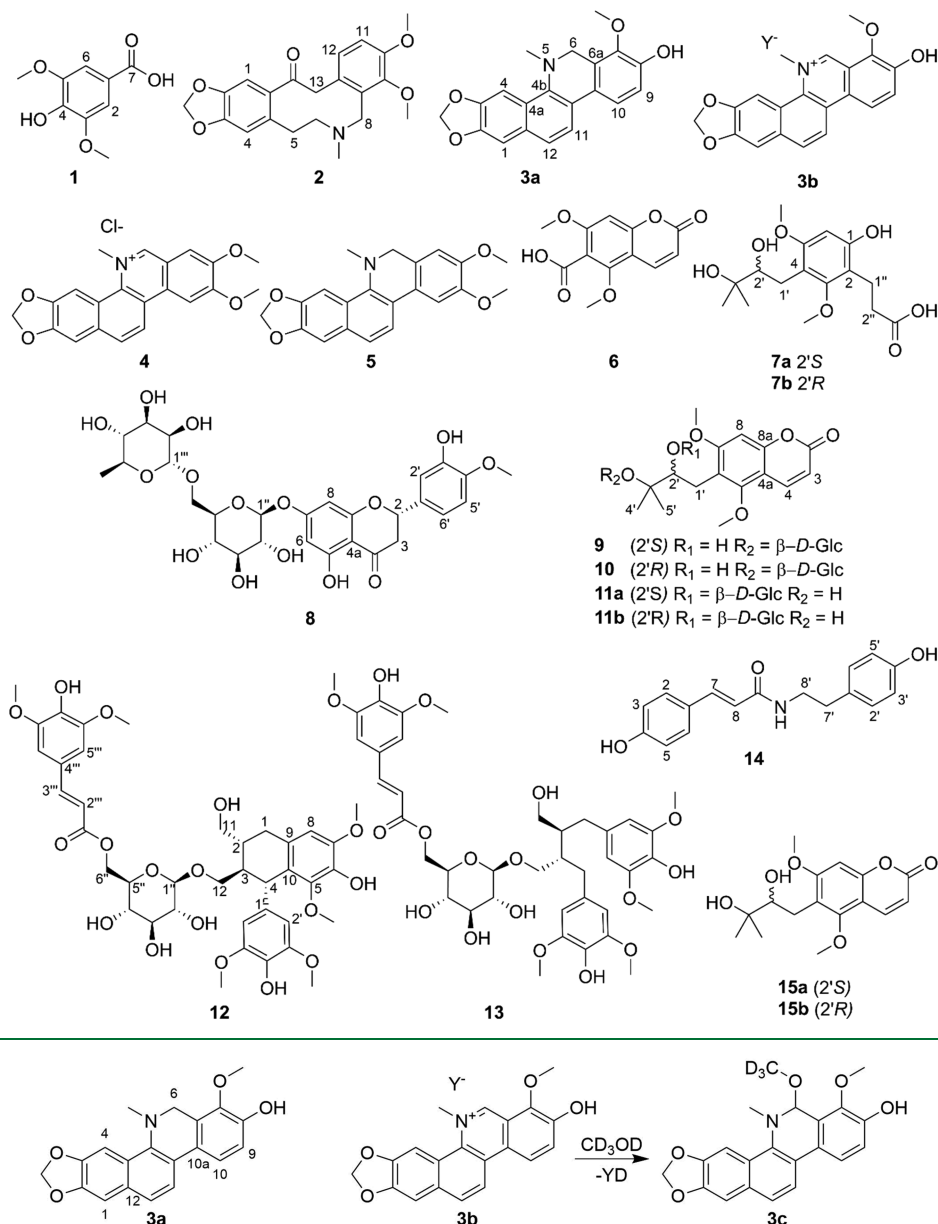


**Figure 1.** Isolated mixture of compounds 3a and 3b and proposed reaction of compound 3b to yield 3c.

with literature data, compound 2 was identified as allocryptopine.<sup>13</sup>

Fagaridine (3b, identical to isofagaridine<sup>14</sup>) was obtained as the major compound in a 4:1 mixture with dihydrofagaridine (3a).<sup>15</sup> Both were identified by comparison of their NMR data (Table S3, Supporting Information) with the literature.<sup>14,15</sup> To prepare fagaridine (3b) as the respective chloride for biological testing, the mixture was passed through an ion-exchange resin. In the resulting compound a change was observed for the chemical shifts of C-6 ( $\delta_C$  86.3) and H-6 ( $\delta_H$  5.53). The presence of a methoxy group at C-6 was supported by an HMBC correlation of H-6 to a carbon at  $\delta_C$  51.8. However, no correlating protons were seen in the HSQC-DEPT spectrum. This suggested the formation of the pseudobase of fagaridine in the presence of methanol-*d*<sub>4</sub> used for the NMR measurements (Figure 1). Indeed, similar reactions have been described before.<sup>16,17</sup>

Compound 4 was identified as nitidine by analysis of its 1D and 2D NMR spectra in DMSO-*d*<sub>6</sub> with trifluoroacetic acid (Table S4, Supporting Information). Nitidine chloride was successively prepared using an ion-exchange resin.<sup>18</sup> The <sup>1</sup>H NMR shifts in DMSO-*d*<sub>6</sub> (Table S4, Supporting Information) and MS data (HRESIMS data *m/z* 348.1223 [M]<sup>+</sup>, calcd for C<sub>21</sub>H<sub>18</sub>NO<sub>4</sub><sup>+</sup>, 348.1230) were in good agreement with published data.<sup>19</sup>

Compound 5 was identified as dihydronitidine (Table S4, Supporting Information).<sup>20,21</sup>

For compound 6, a molecular formula of C<sub>12</sub>H<sub>10</sub>O<sub>6</sub> (HRESIMS data *m/z* 251.0542 [M + H]<sup>+</sup>, calcd for C<sub>12</sub>H<sub>11</sub>O<sub>6</sub><sup>+</sup>, 251.0550) was determined, which, in combination with 1D and 2D NMR data (Table 1), suggested a coumarin. However, no signals for the proposed carboxylic acid moiety at C-6 appeared in the HMBC and <sup>13</sup>C NMR spectra. The compound was methylated with trimethylsilyl diazomethane

**Table 1.**  $^1\text{H}$  and  $^{13}\text{C}$  NMR Spectroscopic Data (500 MHz, Methanol- $d_4$ ) for Compounds **6** and **6a**

position	<b>6</b>		<b>6a</b>	
	$\delta_{\text{C}}$ , type	$\delta_{\text{H}}$ (J in Hz)	$\delta_{\text{C}}$ , type <sup>a</sup>	$\delta_{\text{H}}$ (J in Hz)
2	163.2, C		162.2, C	
3	113.2, CH	6.24, d (9.8)	113.5, CH	6.28, d (9.8)
4	140.9, CH	8.03, d (9.8)	140.0, CH	8.02, d (9.8)
4a	108.2, C		108, C	
5	155.2, C		156.3, C	
6	118.7 <sup>a</sup> , C		115.1, C	
7	161.7, C		161.6, C	
8	96.1, CH	6.74, s	96.3, CH	6.79, s
8a	157.4, C		158.1, C	
11	<sup>c</sup>		167.1, C	
12	63.4, CH <sub>3</sub>	3.99, s	63.7, CH <sub>3</sub>	3.92, s
13	57.1, CH <sub>3</sub>	3.90, s	57.1, CH <sub>3</sub>	3.90, s <sup>b</sup>
14			52.9, CH <sub>3</sub>	3.89, s <sup>b</sup>

<sup>a</sup> $^{13}\text{C}$  extracted from  $^1\text{H}$ - $^{13}\text{C}$  2D inverse-detected experiments.

<sup>b</sup>Overlapping signals. <sup>c</sup>Signal not found.

(TMS-DAM) to obtain methyl ester **6a** (Figure S17, Supporting Information) with a molecular formula of  $\text{C}_{13}\text{H}_{12}\text{O}_6$  (HRESIMS data  $m/z$  265.0706  $[\text{M} + \text{H}]^+$ , calcd for  $\text{C}_{13}\text{H}_{13}\text{O}_6^+$ , 265.0707), and the structure was corroborated by NMR data as the methyl ester of **6**. Thus, toddalic acid (**6**) was confirmed as a new coumarin and only similar to buntasin, another naturally occurring coumarin carboxylic acid found in some *Citrus* species.<sup>22</sup>

The molecular formula of compound **7** was determined as  $\text{C}_{16}\text{H}_{22}\text{O}_7$  (HRESIMS data  $m/z$  327.1437  $[\text{M} - \text{H}]^-$ , calcd for  $\text{C}_{16}\text{H}_{23}\text{O}_7^-$ , 327.1449). NMR data (Table 2) indicated an

**Table 2.**  $^1\text{H}$  and  $^{13}\text{C}$  NMR Spectroscopic Data (500 MHz, Methanol- $d_4$ ) for Compound **7**

position	$\delta_{\text{C}}$ , type	$\delta_{\text{H}}$ (J in Hz)	HMBC
1	156.7, C		
2	114.1, C		
3	159.9, C		
4	113.5, C		
5	158.9, C		
6	96.7, CH	6.30, s	1, 2, 4, 5
7	62.2, CH <sub>3</sub>	3.75, s <sup>a</sup>	3
8	56.1, CH <sub>3</sub>	3.76, s <sup>a</sup>	5
1'	27.2, CH <sub>2</sub>	2.66, dd (13.7, 10.1)	3, 4, 5, 2', 3'
1''		2.86 <sup>a</sup>	3, 4, 5, 2', 3'
2'	79.9, CH	3.56, dd (9.8, 2.8)	1', 3', 4
3'	74.2, C		
4'	25.4, CH <sub>3</sub>	1.23, s <sup>a</sup>	2', 3', 5'
5'	25.8, CH <sub>3</sub>	1.22, s <sup>a</sup>	2', 3', 4'
1''	20.9, CH <sub>2</sub>	2.87 <sup>a</sup>	2, 2'', 3''
2''	35.3, CH <sub>2</sub>	2.54, t (8.2, 8.2)	1'', 3''
3''	178.1, C		

<sup>a</sup>Overlapping signals.

aromatic ring bearing one hydroxy group, two methoxy groups ( $\text{CH}_3$ -7 and  $\text{CH}_3$ -8;  $\delta_{\text{H}}$  3.75 and 3.76), a 2-methylbutan-2,3-diol side chain, and a propionic acid residue (C-3'');  $\delta_{\text{C}}$  178.1). The location of substituents on the aromatic ring were determined with the aid of  $^{13}\text{C}$  NMR and HMBC data, leading to the 2D structure of **7**. To determine the absolute configuration at C-2', an ECD spectrum was recorded and

compared to *ab initio* calculated spectra of the enantiomers (Figure S3(B), Supporting Information). The measured ECD spectrum had a low signal-to-noise ratio and showed no significant features of an expected  $\pi \rightarrow \pi^*$  transition at 220 nm hinting at a scalemic mixture. The enantiomers were subsequently separated by chiral-phase HPLC. ECD spectra (Figure S3(B), Supporting Information) and the specific rotations of the single enantiomers were recorded. The specific rotations and ECD values for compound **7b** were smaller than could be expected. This was most likely due to an impurity not observed in the NMR. Comparison to the *ab initio* calculated ECD spectra identified **7a** as  $(-)$ -(2'*S*)-toddanolic acid and **7b** as  $(+)$ -(2'*R*)-toddanolic acid.

The 2D structure of compound **8** (Table S5, Supporting Information) corresponded to that of hesperidin.<sup>23,24</sup>

Compounds **9** and **10** were identified by 1D and 2D NMR data analysis as toddalolactones bearing a sugar moiety at C-3'. Hydrolysis and subsequent GCMS analysis of the sugar afforded D-glucose in both cases. Therefore, **9** and **10** were epimers at C-2', and this was corroborated by a difference in  $^{13}\text{C}$  chemical shifts of  $\text{CH}_3$ -4' ( $\delta_{\text{C}}$  21.9 in **9** and  $\delta_{\text{C}}$  23.0 in **10**) and  $\text{CH}_3$ -5' ( $\delta_{\text{C}}$  24.0 in **9** and  $\delta_{\text{C}}$  23.4 in **10**). Compound **9** showed a specific rotation of  $[\alpha]_{\text{D}}^{25} -45$  and  $[\alpha]_{\text{D}}^{25} -2.5$  for **10**. The (2'*S*)-epimer (**9**) was reported earlier by Lin et al. with a specific rotation of  $[\alpha]_{\text{D}}^{25} -44$ .<sup>25</sup> In a recent publication, however, the (2'*R*)-epimer **10** was reported as the "enantiomer" of the (2'*S*)-epimer, with  $^{13}\text{C}$  NMR data virtually identical to those of Lin's (2'*S*)-epimer, but with exactly opposite specific rotations.<sup>26</sup> This was highly unexpected in light of our data, and the absolute configuration of C-2' in both compounds was therefore examined in detail.

The absolute configuration at C-2' was determined by ECD. The experimental spectra of **9** and **10** showed Cotton effects (CEs) at 225, 253, and 330 nm with opposite signs. In the calculated spectra (Figure 2) the sign for the CE at 330 nm was negative for both epimers. Therefore, the CEs at 225 and 253 nm were used for the assignment. The two negative CEs measured for **9** were in good agreement with the calculated CEs for (2'*S*)-toddalolactone 3'-*O*- $\beta$ -D-glucopyranoside. The spectrum measured for **10** showed positive CEs at 225 and 253 nm. The observed CE at 225 nm matched with a positive CE

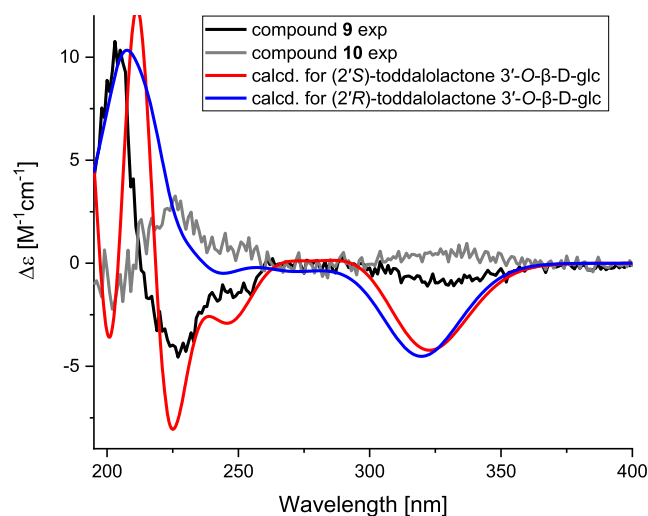
**Figure 2.** Comparison of experimental and calculated ECD spectra of compounds **9** and **10** in MeOH (calcd spectrum shifted +5 nm).

Table 3. <sup>1</sup>H and <sup>13</sup>C NMR Spectroscopic Data (500 MHz, Methanol-*d*<sub>4</sub>) for Compounds 9, 10, and 11

pos.	9		10		11	
	$\delta_C$ , type	$\delta_H$ (J in Hz)	$\delta_C$ , type	$\delta_H$ (J in Hz)	$\delta_C$ , type	$\delta_H$ (J in Hz)
2	163.5, C		163.5, C		163.7, C	
3	112.7, CH	6.22, d (9.8)	112.7, CH	6.20, d (9.6)	112.6, CH	6.21, d (9.5)
4	141.3, CH	8.00, d (9.8)	141.4, CH	7.97, d (9.6)	141.6, CH	7.98, d (9.5)
4a	108.5, C		108.5, C		108.5, C	
5	157.7, C		157.8, C		157.9, C	
6	120.3, C		120.4, C		120.0, C	
7	163.7, C		163.9, C		164.1, C	
8	96.4, CH	6.72, s	96.4, CH	6.69, s	96.3, CH	6.71, s
8a	156.2, C		156.3, C		156.4, C	
9	64.0, CH <sub>3</sub>	3.90, s <sup>a</sup>	64.0, CH <sub>3</sub>	3.88, s <sup>a</sup>	64.2, CH <sub>3</sub>	3.90, s <sup>a</sup>
10	56.9, CH <sub>3</sub>	3.91, s <sup>a</sup>	56.9, CH <sub>3</sub>	3.88, s <sup>a</sup>	56.9, CH	3.90, s <sup>a</sup>
1'	27.2, CH <sub>2</sub>	2.90, dd (13.6, 10.1)	27.2, CH <sub>2</sub>	2.89, dd (13.7, 9.8)	27.0, CH <sub>2</sub>	2.98, dd (13.7, 10.0)
1''		2.79, dd (13.6, 2.0)		2.76, dd (13.7, 2.4)		2.72, d (13.7)
2'	77.6, CH	3.81 <sup>a</sup>	77.2, CH	3.79 <sup>a</sup>	88.1, CH	3.87 <sup>a</sup>
3'	82.0, C		81.6, C		75.1, C	
4'	21.9, CH <sub>3</sub>	1.36, s <sup>a</sup>	23.0, CH <sub>3</sub>	1.34, s <sup>a</sup>	24.3, CH <sub>3</sub>	1.30, s
5'	24.0, CH <sub>3</sub>	1.35, s <sup>a</sup>	23.4, CH <sub>3</sub>	1.35, s <sup>a</sup>	26.6, CH <sub>3</sub>	1.25, s
1''	98.7, CH	4.57, d (7.6) <sup>a</sup>	98.3, CH	4.55, d (7.6) <sup>a</sup>	106.1, CH	4.20, d (7.0)
2''	75.3, CH	3.22, dd (8.4, 7.6)	75.5, CH	3.19, dd (9.5, 7.6)	76, CH	3.06 <sup>a</sup>
3''	78.1, CH	3.4, dd (8.4, 8.4)	78.3, CH	3.38, dd (9.5, 7.9)	78.1, CH	3.23 <sup>a</sup>
4''	71.7, CH	3.32 <sup>a</sup>	71.8, CH	3.31 <sup>a</sup>	71.7, CH	3.06 <sup>a</sup>
5''	77.8, CH	3.29 <sup>a</sup>	77.9, CH	3.28 <sup>a</sup>	77.3, CH	2.90, m
6''	62.8, CH <sub>2</sub>	3.65, dd (11.7, 5.0)	62.9, CH <sub>2</sub>	3.66, dd (11.7, 4.7)	62.9, CH <sub>2</sub>	3.22 <sup>a</sup>
6'''		3.82, m <sup>a</sup>		3.82 <sup>a</sup>		3.26 <sup>a</sup>

<sup>a</sup>Overlapping signals.

in the calculated spectrum of (2'*R*)-toddalolactone 3'-*O*- $\beta$ -*D*-glucopyranoside, but no interpretable CE was seen in the calculated spectrum at 253 nm. To corroborate the assignments, compounds **9** and **10** were subjected to acid hydrolysis with HCl.<sup>25</sup> This led to an almost quantitative formation of ketone **9a** and, via a rearrangement, to aldehyde **9b** (Figures S18 and S81–S84, Supporting Information) and a small amount of the aglycones. Using chiral-phase chromatography on a Daicel Chiralpak IG column, the aglycone of **9** was identified as (2'*S*)-toddalolactone, and that of **10** as (2'*R*)-toddalolactone (Figure S128, Supporting Information). Enzymatic hydrolysis of **9** and **10** with cellulase was used to obtain the aglycones in sufficient amounts for ECD and specific rotation (SR) analysis (Figures S123–S126, Supporting Information). ECD identified the aglycone of **9** as the (2'*S*) enantiomer, and the one from **10** as the (2'*R*)-enantiomer (Figure S8, Supporting Information). Collectively, compound **9** was identified as (2'*S*)-toddalolactone 3'-*O*- $\beta$ -*D*-glucopyranoside and compound **10** as (2'*R*)-toddalolactone 3'-*O*- $\beta$ -*D*-glucopyranoside. Coumarin **10** has been recently reported, but the assignment of its absolute configuration was solely based on OR data and a questionable correlation with previously known glucoside **9**.<sup>26</sup>

Compound **11** had a molecular formula of C<sub>22</sub>H<sub>30</sub>O<sub>11</sub> (HRESIMS data *m/z* 493.1672 [M + Na]<sup>+</sup>, calcd for C<sub>22</sub>H<sub>30</sub>O<sub>11</sub>Na<sup>+</sup>, 493.1680), and 1D and 2D NMR data (Table 3) identified it as toddalolactone 2'-*O*- $\beta$ -*D*-glucopyranoside.<sup>26</sup> As the absolute configuration of **11** was hitherto only based on SR data, an ECD spectrum was recorded and compared to calculated spectra of both possible epimers (Figure S9, Supporting Information). However, the calculated spectra were highly similar; thus the analysis was inconclusive. Acidic hydrolysis of **11** afforded the aglycone together with the

respective ketone and aldehyde (Figure S18, Supporting Information). The aglycone was identified via chiral-phase HPLC as (2'*S*)-toddalolactone (Figure S128, Supporting Information), and compound **11** was conclusively identified as (2'*S*)-toddalolactone 2'-*O*- $\beta$ -*D*-glucopyranoside.

A molecular formula of C<sub>39</sub>H<sub>48</sub>O<sub>17</sub> was determined for compound **12** (HRESIMS data *m/z* 811.2758 [M + Na]<sup>+</sup>, calcd for C<sub>39</sub>H<sub>48</sub>O<sub>17</sub>Na<sup>+</sup>, 811.2784). Using 1D and 2D NMR data, compound **12** was identified as hazaleanin B (Table S7, Supporting Information), which was previously reported from *Fagara rhetza* (Rutaceae)<sup>27</sup> and Zhuyeqing Liquor.<sup>28</sup> ECD analysis corroborated the published absolute configuration as (2*R*,3*R*,4*S*)-hazaleanin B (Figure S11, Supporting Information).

Compound **13** had a molecular formula of C<sub>39</sub>H<sub>50</sub>O<sub>17</sub> (HRESIMS data *m/z* 813.2916 [M + Na]<sup>+</sup>, calcd for C<sub>39</sub>H<sub>50</sub>O<sub>17</sub>Na<sup>+</sup>, 813.2940). By 1D and 2D NMR analysis **13** was identified as hazaleanin A.<sup>27</sup> ECD data analysis was used to independently confirm the absolute configuration. Owing to the high conformational flexibility of **13**, the conformational analysis was performed not in bulk but in explicit MeOH by means of molecular dynamics simulations. A comparison of the experimental and calculated spectra (spectra in Figure S13, selected conformers in Figures S19–S22, Supporting Information) resulted in the assignment of **13** as (2*S*,3*S*)-hazaleanin in accordance with the findings of Shibuya et al.<sup>27</sup> This is the first report of the presence of hazaleanins A and B in *T. asiatica*.

Compound **14** was identified by 1D and 2D NMR data as *p*-coumaroyltyramine (Table S8, Supporting Information).<sup>29</sup>

Compound **15** had a molecular formula of C<sub>16</sub>H<sub>20</sub>O<sub>6</sub> (HRESIMS data *m/z* 309.1329 [M + Na]<sup>+</sup>, calcd for C<sub>16</sub>H<sub>20</sub>O<sub>6</sub>Na<sup>+</sup>, 309.1333), and 1D and 2D NMR data (Table S9, Supporting Information) identified the compound as

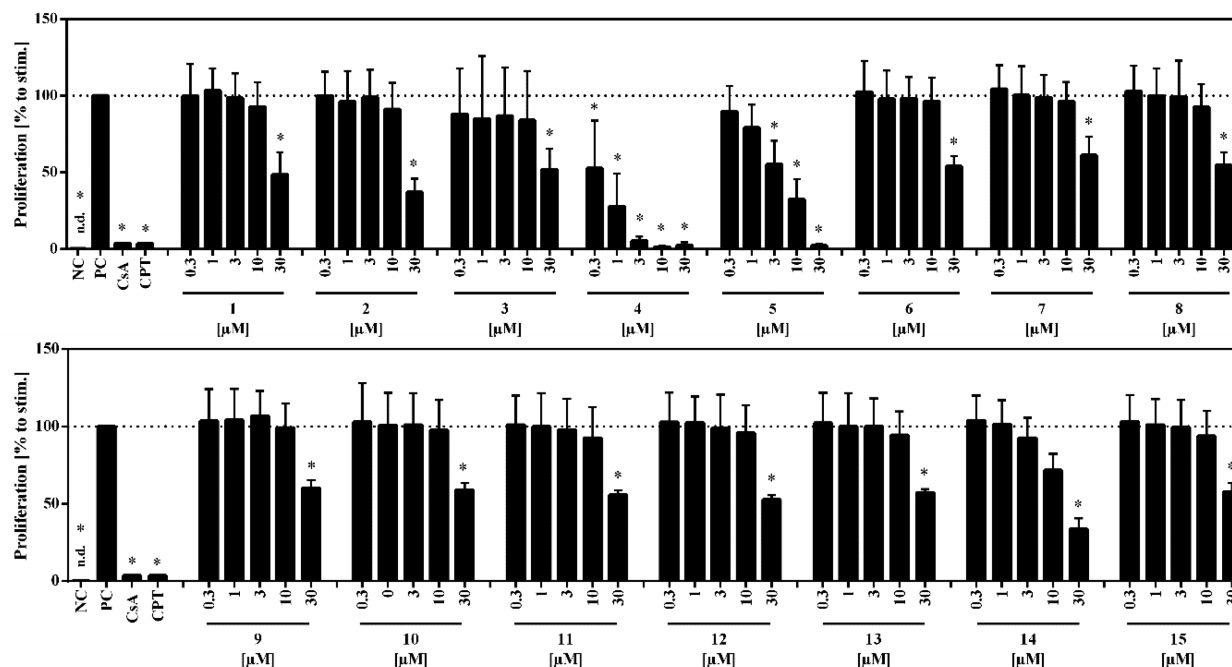


**Figure 3.** Inhibitory effects of compounds 1–15 on the proliferation of human T lymphocytes. Human PBMCs ( $2 \times 10^5$ ) were stained with CFSE and stimulated with anti-CD3 and anti-CD28 monoclonal antibodies (mAbs, 100 ng/mL each). Unstimulated cells served as a negative control (NC). Afterward, cells were incubated for 72 h in the presence of medium (PC), cyclosporin A (CsA; 4.16  $\mu$ M), camptothecin (CPT; 300  $\mu$ M), or compounds 1–15 at concentrations between 0.3 and 30  $\mu$ M. Cell division was analyzed by flow cytometry. The percentage of proliferating cells was normalized to the stimulated control and depicted as mean  $\pm$  standard deviation.  $n = 3$ . \* $p < 0.05$ .

toddalolactone.<sup>25,30</sup> The negative sign of the specific rotation suggested (2′*S*)-toddalolactone (**15a**).<sup>25</sup> This was supported by the ECD spectrum, which was compared to the calculated spectra of both enantiomers **15a** and **15b** (Figure S15, Supporting Information). The SR of **15** ( $[\alpha]_D^{25} -10$ ) compared to (2′*S*)-toddalolactone (**15a**) obtained by enzymatic hydrolysis of **9** ( $[\alpha]_D^{25} -51$ ) indicated the enantiomeric excess of **15a** as 20%. This analysis was corroborated by a <sup>1</sup>H NMR experiment in the presence of the shift reagent Eu(hfc)<sub>3</sub><sup>31</sup> (29% enantiomeric excess of **15a**) and chiral-phase HPLC on a Daicel Chiralpak IG column (25% enantiomeric excess of **15a**).

In conclusion, a total of 15 compounds were isolated from the MeOH extract of *T. asiatica*, of which toddalic acid (**6**) and toddanolic acid (**7**) were new natural products. Although compound **10**, the 2′-epimer of **9**, was reported recently, we provide here the first full structural assignment and spectroscopic data. The co-occurrence of **9** and **10** indicates that both enantiomers of toddalolactone are naturally present in the plant.<sup>32</sup> The carboxylic moiety at C-6 in coumarin **6** is unusual from a biosynthetic perspective, and only one similar naturally occurring coumarin has been reported so far.<sup>22</sup> Toddanolic acid (**7**) is structurally related to toddalolactone (**15**). An artifactual formation of **7** can be ruled out given that an opening of the lactone ring and reduction of the double bond would require conditions (e.g., basic pH, metal catalyst, and NaBH<sub>4</sub>) far from the ones used during the isolation.<sup>33,34</sup>

Compounds 1–15 were tested for their ability to suppress the proliferation of stimulated human primary T lymphocytes in vitro. Compounds 1–3 and 6–15 showed slight inhibition of T cell proliferation at the highest test concentration of 30  $\mu$ M. Compounds 4 and 5 concentration-dependently inhibited T cell proliferation with IC<sub>50</sub>'s of 0.4  $\mu$ M ( $R^2 = 0.7$ ) and 6.7  $\mu$ M ( $R^2 = 0.9$ ), respectively (Figure 3). Cytotoxic effects were

detected only at 10 and 30  $\mu$ M concentrations for compound 4 and at 30  $\mu$ M concentration for 5. Nitidine chloride (**4**) has been previously found to modulate reactive microgliosis after traumatic brain injury at 0.1  $\mu$ M, and inhibition of the ERK and NF- $\kappa$ B signaling pathways in microglia cells was reported.<sup>35</sup> Inhibition of T cell proliferation by nitidine chloride (**4**) observed in our study could thus be caused by inhibition of these pathways. Nitidine chloride reportedly also induces apoptosis in HCT116 human colorectal cancer cells via inhibition of ERK.<sup>36</sup> In conclusion, nitidine chloride (**4**) is a potential lead, with inhibition of T cell proliferation at sub-micromolar concentrations and an apparent cytotoxicity only at a 25-fold higher concentration. This possibility was also corroborated by a patent (CN102008474B) filed for the use of nitidine in the treatment of autoimmune diseases and resisting transplant rejection.<sup>37</sup> The related dihydronitidine (**5**) has been reported to selectively induce apoptosis in various tumor cell lines when tested at low micromolar concentrations.<sup>38</sup>

## EXPERIMENTAL SECTION

**General Experimental Procedures.** Optical rotations were measured at concentrations between 0.4 and 1 mg/mL in MeOH on a PerkinElmer 341 polarimeter with a 10 cm microcell. UV and ECD spectra were recorded in MeOH (50–150  $\mu$ g/mL) on a Chirascan CD spectrometer using 1 mm path precision cells (110 QS, Hellma Analytics). NMR data were recorded on a Bruker Avance III NMR spectrometer operating at 500.13 MHz for <sup>1</sup>H and 125.77 MHz for <sup>13</sup>C nuclei. <sup>1</sup>H NMR, COSY, HSQC, HMBC, and NOESY spectra were measured at 23 °C in a 1 mm TXI probe with a z-gradient. <sup>13</sup>C NMR/DEPTQ spectra were recorded at 23 °C in 3 mm tubes using a 5 mm BBI probe. For compound 2, <sup>1</sup>H, COSY, HSQC, and HMBC spectra were also recorded at 60 °C. All spectra were analyzed using Bruker TopSpin 3.5 and ACDLabs NMR Workbook software suites. NMR spectra were recorded in CDCl<sub>3</sub> (Sigma-Aldrich), methanol-*d*<sub>4</sub>, DMSO-*d*<sub>6</sub>, or TFA (all Armar Chemicals). HPLC-PDA-ELSD-ESIMS

data were recorded in the positive and negative mode on a Shimadzu LC-MS/MS 8030 triple quadrupole ESIMS system connected via a T-splitter (1:10) to a Shimadzu HPLC system consisting of a degasser, binary high-pressure mixing pump, autosampler, column oven, and diode array detector, and via a T-split to an Alltech 3300 ELSD detector. Data were acquired and processed with the LabSolution software suite. Semipreparative HPLC separations were carried out with an Agilent HP 1100 Series system consisting of a quaternary pump, autosampler, column oven, and a diode array detector (G1315B). Preparative HPLC separations were carried out using Agilent 1290 Infinity II preparative binary pumps and an Agilent 1100 DAD detector in line with an Agilent 6120 Quadrupole LC/MS detector. The column effluent was collected via an active split (100:1) between HPLC columns and detectors. Chemstation software was used for data acquisition and processing. Waters SunFire C<sub>18</sub> (3.5  $\mu$ m, 3.0  $\times$  150 mm i.d., equipped with a guard column 10  $\times$  3.0 mm i.d.), SunFire Prep C<sub>18</sub> (5  $\mu$ m, 10  $\times$  150 mm i.d., equipped with a guard column 10  $\times$  10 mm i.d.), and SunFire Prep C<sub>18</sub> OBD (5  $\mu$ m, 30  $\times$  150 mm i.d., equipped with a guard column 10  $\times$  20 mm i.d.) columns were used for reverse-phase analytical, semipreparative, and preparative separations, respectively. Chiral-phase HPLC separations were performed at a flow rate of 1 mL/min on either a Daicel Chiralpak IG column (5  $\mu$ m, 250  $\times$  4.6 mm) eluted with 20% CH<sub>3</sub>CN in H<sub>2</sub>O for 10 min or a Daicel Chiralpak IF column (5  $\mu$ m, 250  $\times$  4.6 mm) eluted with 20% CH<sub>3</sub>CN in H<sub>2</sub>O, both containing 0.1% formic acid (FA), for 10 min. HPLC-grade MeOH, CH<sub>3</sub>CN (Scharlau Chemie), and water from a Milli-Q water purification system (Merck Millipore) were used for HPLC separations. The mobile phase used for analytical HPLC contained 0.1% FA. Technical-grade solvents purified by distillation were used for extraction, open column chromatography, and CPC separations. Silica gel (15–40  $\mu$ m, Merck) and C<sub>18</sub> modified silica (RP-18 LiChroprep 25–40  $\mu$ m) were used for open column chromatography. HRESIMS data were measured on an LQT XL Orbitrap mass spectrometer (Thermo Scientific) coupled to a Shimadzu LC-MS system equipped with a Waters SunFire C<sub>18</sub> column (3.5  $\mu$ m, 3.0  $\times$  150 mm i.d., equipped with a guard column 10  $\times$  3.0 mm i.d.). Trimethylsilyldiazomethane was purchased from Tokio Chemical Industry, and Lewatit MonoPlus SP 112 (Na<sup>+</sup> form), Eu(hfc)<sub>3</sub>, and cellulase enzyme blend were from Sigma-Aldrich, Germany.

**Plant Material.** *T. asiatica* roots were purchased from Bozhou Swan Commerce and Trade Co., Ltd. (Bozhou, China) in January 2018. A voucher specimen (number 0 1026) has been deposited at the Division of Pharmaceutical Biology, University of Basel, Switzerland.

**Microfractionation.** Microfractionation of *T. asiatica* MeOH extract was carried out by analytical RP-HPLC on an LC-MS 8030 system (Shimadzu) connected with an FC 204 fraction collector (Gilson). A solution of 10 mg/mL extract in DMSO was prepared, and three injections were performed: 2  $\times$  30  $\mu$ L for microfractionation, using only the PDA (0.6 mg of extract in total), and 1  $\times$  10  $\mu$ L with PDA-ELSD-ESIMS detectors without microfractionation. Water containing 0.1% FA (solvent A) and CH<sub>3</sub>CN with 0.1% FA (B) were used as a mobile phase. A linear gradient from 5 to 60% B in 30 min was followed by 5 min at 100% B. Microfractions of 1 min each were collected from the beginning of minute 2 to the end of minute 34. Corresponding microfractions of two successive injections were collected into the same wells of a 96-deep-well plate. The plates were dried in a Genevac EZ-2 evaporator.

**Extraction and Isolation.** *T. asiatica* roots were ground with a Retsch ZM1 centrifugal mill. A 740 g amount of the powdered roots was extracted with 4  $\times$  2.2 L of DCM over 24 h. The remaining plant material was extracted with 3  $\times$  2.2 L of MeOH over 24 h. The combined MeOH extracts were dried in vacuo and freeze-dried to afford 38.7 g of dry residue. A 35.7 g amount of MeOH extract was subjected to liquid–liquid partitioning using a two-phase system containing 928 mL of CHCl<sub>3</sub>, 500 mL of MeOH, and 570 mL of H<sub>2</sub>O. After removal of the organic phase, the aqueous phase was successively extracted with a mixture of 800 mL of CHCl<sub>3</sub> and 200 mL of MeOH, a mixture of 500 mL of CHCl<sub>3</sub> and 500 mL of MeOH,

and a mixture of 1500 mL of CHCl<sub>3</sub> and 500 mL of MeOH. The organic layers were combined and dried *in vacuo*, yielding 17.3 g of an enriched fraction. A precipitate at the interface of the aqueous and the organic layers was collected separately, filtered, and washed with cold CHCl<sub>3</sub> and MeOH to give 548 mg of **8**. Aliquots of the enriched fraction (1.9 to 3.0 g per run) were subjected to centrifugal partition chromatography (CPC) using CHCl<sub>3</sub>/MeOH/H<sub>2</sub>O (25:30:20) at a flow rate of 5 mL/min in descending mode. Six fractions (A–F) were collected, and a switch to ascending mode gave four additional fractions (G–K). Fraction E (559 mg) was separated on a C<sub>18</sub> column (25–40  $\mu$ m, 5  $\times$  47 cm) connected to an Interchim Puriflash 4100 system [water + 0.1% FA (A), CH<sub>3</sub>CN + 0.1% FA (B); 27% B (0–5 min) 27  $\rightarrow$  44% B (5–202 min), 44  $\rightarrow$  100% (202–220 min), 100% (220–245 min); flow rate 22 mL/min; sample dissolved in 1.3 mL of MeOH], and fractions E<sub>1</sub>–E<sub>16</sub> were obtained. E<sub>6</sub> (6 mg) was purified by semipreparative RP HPLC [CH<sub>3</sub>CN + 0.1% FA (A), H<sub>2</sub>O + 0.1% FA (B); 18% B (0–20 min) 18  $\rightarrow$  20% B (20–22 min), 20  $\rightarrow$  100% (22–26 min), 100% (26–31 min); flow rate 4 mL/min; concentration 50 mg/mL in MeOH, injection volume 10–40  $\mu$ L] to yield dihydronitidine (**5**, 0.6 mg). The rest of fraction E (600 mg) was chromatographed on a silica gel column (15–40  $\mu$ m; 3.5  $\times$  35 cm) connected to an Interchim Puriflash 4100 system [CHCl<sub>3</sub> (A), MeOH (B); 100% A (0–5 min) 0  $\rightarrow$  2% B (5–10 min), 2  $\rightarrow$  5% (10–20 min), 5  $\rightarrow$  30% (20–110 min), 30  $\rightarrow$  50% (110–175 min), 50  $\rightarrow$  55% (175–190 min), 55  $\rightarrow$  57% (190–191 min), 57  $\rightarrow$  100% (191–205 min), 100% (205–260 min); flow rate 20 mL/min; solid state introduction, with the sample adsorbed on 3 g of silica gel (63–200  $\mu$ m, Merck)], and 24 fractions (EA–EX) were obtained. Fraction EL (36 mg) was separated by preparative RP HPLC [CH<sub>3</sub>CN + 0.1% FA (A), H<sub>2</sub>O + 0.1% FA (B); 15% B (0–24 min) 15  $\rightarrow$  25% B (24–35 min), 25  $\rightarrow$  35% B (35–40 min), 35  $\rightarrow$  60% B (40–45 min), 60  $\rightarrow$  100% B (45–47 min), flow rate 25 mL/min; concentration 90 mg/mL in MeOH, injection volume 390  $\mu$ L] to afford a mixture of **3a** and **3b** (3.5 mg). Fraction EN (9.3 mg) was recrystallized from MeOH/H<sub>2</sub>O (1:2) to obtain syringic acid (**1**, 4.5 mg). Fraction EP (22 mg) was separated by preparative RP HPLC [CH<sub>3</sub>CN + 0.1% FA (A), H<sub>2</sub>O + 0.1% FA (B); 15% B (0–3 min) 30  $\rightarrow$  35% B (3–16 min), 35  $\rightarrow$  100% (16–20 min); flow rate 20 mL/min; concentration 55 mg/mL in MeOH/H<sub>2</sub>O (1:3); injection volume 400  $\mu$ L], and fractions EP<sub>1</sub>–EP<sub>4</sub> were collected. EP<sub>3</sub> (5.8 mg) was purified by semipreparative RP HPLC [CH<sub>3</sub>CN + 0.1% FA (A), H<sub>2</sub>O + 0.1% FA (B); 24% B (0–20 min) 24  $\rightarrow$  100% B (20–22 min), 100% B (22–27 min), flow rate 4 mL/min; concentration 2.5 mg/mL MeOH/H<sub>2</sub>O (1:1), 3 injections with injection volumes 40–70  $\mu$ L] to afford **12** (3.6 mg) and **13** (1.5 mg). Fraction EQ (60 mg) was separated by preparative RP HPLC [CH<sub>3</sub>CN + 0.1% FA (A), H<sub>2</sub>O + 0.1% FA (B); 23% B (0–30 min) 23  $\rightarrow$  100% B (30–31 min), 100% B (31–36 min); flow rate 20 mL/min; concentration 83 mg/mL in MeOH/H<sub>2</sub>O (1:3); 2 injections of 300–400  $\mu$ L] to afford **9** (20 mg), **10** (11 mg), and **11** (5.1 mg). Fraction ET (55 mg) was dissolved in 700  $\mu$ L MeOH/H<sub>2</sub>O (3:1), and the supernatant was subjected to preparative HPLC [CH<sub>3</sub>CN + 0.1% FA (A), H<sub>2</sub>O + 0.1% FA (B); 13% B (0–2 min), 13  $\rightarrow$  25% B (2–32 min), 25  $\rightarrow$  29% (32–42 min), 29  $\rightarrow$  60% (42–50 min), 60% (50–52 min), 60  $\rightarrow$  100% B (52–55 min), flow rate 20 mL/min; concentration 75 mg/mL in MeOH/H<sub>2</sub>O (3:1); injection volume 700  $\mu$ L] to yield **2** (1.6 mg). Fraction EV (22 mg) was separated by preparative RP HPLC [CH<sub>3</sub>CN + 0.1% FA (A), H<sub>2</sub>O + 0.1% FA (B); 21% B (0–3 min) 21  $\rightarrow$  29% B (3–24 min), 29  $\rightarrow$  100% (24–30 min), flow rate 20 mL/min; concentration 55 mg/mL in MeOH/H<sub>2</sub>O (1:1); injection volume 400  $\mu$ L] to afford fractions EV<sub>1</sub>–EV<sub>5</sub>. Fraction EV<sub>1</sub> (5.8 mg) was purified by semipreparative RP HPLC [CH<sub>3</sub>CN + 0.1% FA (A), H<sub>2</sub>O + 0.1% FA (B); 11% B (0–30 min) 11  $\rightarrow$  100% B (30–32 min), 100% B (32–38 min), flow rate 4 mL/min; concentration 33 mg/mL in MeOH/H<sub>2</sub>O (1:2), 2 injections of 60  $\mu$ L], to afford **6** (1.0 mg) and **7** (1.5 mg). As compound **7** was obtained as a scalemic mixture of both enantiomers, the enantiomers **7a** and **7b** were separated via chiral-phase HPLC on a Daicel Chiralpak IF column [CH<sub>3</sub>CN + 0.1% FA (A), H<sub>2</sub>O + 0.1% FA (B); 20% B (0–10 min), flow rate 1 mL/min; concentration of 5 mg/mL; 8 injections with 10  $\mu$ L]. Compound **7b**

eluted at 7.3 min, and compound **7a** at 8.4 min. Fraction EW (58 mg) was dissolved in 580  $\mu$ L MeOH and 10  $\mu$ L of FA and subjected to preparative RP HPLC [CH<sub>3</sub>CN (A), H<sub>2</sub>O (B); 16% B (0–48 min), 16  $\rightarrow$  100% B (48–53 min); flow rate 25 mL/min; concentration of 90 mg/mL; injection volume 550  $\mu$ L], to afford **4** (10.1 mg). The hydrochloride of **4** was prepared via filtration over Lewatit MonoPlus SP 112 resin.

**Syringic acid (1)**: white solid; <sup>1</sup>H and <sup>13</sup>C NMR, see Table S1, Supporting Information; HRESIMS  $m/z$  181.0489 [M + H – H<sub>2</sub>O]<sup>+</sup> (calcd for C<sub>9</sub>H<sub>9</sub>O<sub>4</sub><sup>+</sup>, 181.0495).

**Allocryptopine (2)**: colorless solid; <sup>1</sup>H and <sup>13</sup>C NMR, see Table S2, Supporting Information; HRESIMS  $m/z$  370.1646 [M + H]<sup>+</sup> (calcd for C<sub>21</sub>H<sub>24</sub>NO<sub>5</sub><sup>+</sup>, 370.1649).

**Fagaridine and dihydrofagaridine (3b and 3a)**: red solid; <sup>1</sup>H and <sup>13</sup>C NMR, see Table S3, Supporting Information; HRESIMS  $m/z$  334.1059 [M]<sup>+</sup> (calcd for C<sub>20</sub>H<sub>16</sub>NO<sub>4</sub><sup>+</sup>, 334.1074).

**Compound 3b**: <sup>1</sup>H and <sup>13</sup>C NMR, see Table S3, Supporting Information.

**Nitidine chloride (4)**: yellow solid; <sup>1</sup>H and <sup>13</sup>C NMR, see Table S4, Supporting Information; HRESIMS  $m/z$  338.1223 [M]<sup>+</sup> (calcd for C<sub>21</sub>H<sub>18</sub>NO<sub>4</sub><sup>+</sup>, 338.1230).

**Dihydranitidine (5)**: light yellow solid; <sup>1</sup>H and <sup>13</sup>C NMR, see Table S4, Supporting Information; HRESIMS  $m/z$  348.1220 [M – H]<sup>+</sup> (calcd for C<sub>21</sub>H<sub>18</sub>NO<sub>4</sub><sup>+</sup>, 348.1230) and  $m/z$  334.1064 [M – CH<sub>3</sub>]<sup>+</sup> (calcd for C<sub>20</sub>H<sub>16</sub>NO<sub>4</sub><sup>+</sup>, 334.1074).

**Toddalic acid (6)**: colorless solid; UV  $\lambda_{\max}$  (MeOH) (log  $\epsilon$ ) 206 (4.4) nm, 323 (3.9) nm; <sup>1</sup>H and <sup>13</sup>C NMR, see Table 1; HRESIMS  $m/z$  251.0542 [M + H]<sup>+</sup> (calcd for C<sub>12</sub>H<sub>11</sub>O<sub>6</sub><sup>+</sup>, 251.0550).

**Compound 6a**: colorless solid; <sup>1</sup>H and <sup>13</sup>C NMR, see Table 1; HRESIMS  $m/z$  265.0706 [M + H]<sup>+</sup> (calcd for C<sub>13</sub>H<sub>13</sub>O<sub>6</sub><sup>+</sup>, 265.0707).

**Toddanolic acid (7)**: colorless solid; [ $\alpha$ ]<sub>D</sub><sup>25</sup> –12 (c 0.07 g/100 mL, MeOH); UV  $\lambda_{\max}$  (MeOH) (log  $\epsilon$ ) 204 (4.1), 281 (3.0) nm; ECD (MeOH, c 0.97 mM, 0.1 cm);  $\Delta\epsilon$  +1.49 (204 nm), –0.8 (230 nm); <sup>1</sup>H and <sup>13</sup>C NMR, see Table 2, Supporting Information; HRESIMS  $m/z$  327.1437 [M – H]<sup>–</sup> (calcd for C<sub>16</sub>H<sub>23</sub>O<sub>7</sub><sup>–</sup>, 327.1449).

(–)-(2′S)-Toddanolic acid (**7a**): colorless solid; [ $\alpha$ ]<sub>D</sub><sup>25</sup> –20 (c 0.03 g/100 mL, MeOH); UV  $\lambda_{\max}$  (MeOH) (log  $\epsilon$ ) 204 (4.5), 281 (3.3) nm; ECD (MeOH, c 0.48 mM, 0.1 cm);  $\Delta\epsilon$  –3.4 (205 nm), –1.2 (231 nm), –0.5 (273 nm).

(+)-(2′R)-Toddanolic acid (**7b**): colorless solid; [ $\alpha$ ]<sub>D</sub><sup>25</sup> 32 (c 0.02 g/100 mL, MeOH); UV  $\lambda_{\max}$  (MeOH) (log  $\epsilon$ ) 204 (4.5), 282 (3.4) nm; ECD (MeOH, c 0.32 mM, 0.1 cm);  $\Delta\epsilon$  +8.0 (205 nm), +2.6 (232 nm), +1.1 (275 nm).

(2′S)-Hesperidin (**8**): pale yellow solid; UV  $\lambda_{\max}$  (MeOH) (log  $\epsilon$ ) 200 (4.8), 224 (4.5), 283 (4.3), 331 (3.6) nm; ECD (MeOH, c 0.32 mM, 0.1 cm);  $\Delta\epsilon$  +20.2 (200 nm) +11.0 (223 nm), –10.4 (289 nm), +2.5 (334 nm); <sup>1</sup>H and <sup>13</sup>C NMR, see Table S5, Supporting Information; HRESIMS  $m/z$  633.1778 [M + Na]<sup>+</sup> (calcd for C<sub>28</sub>H<sub>34</sub>NaO<sub>15</sub><sup>+</sup>, 633.1790) ( $m/z$  633.1778 [M + Na]<sup>+</sup>, calcd for C<sub>28</sub>H<sub>34</sub>NaO<sub>15</sub><sup>+</sup>, 633.1790).

(2′S)-Toddalolactone 3′-O- $\beta$ -D-glycopyranoside (**9**): yellow solid; [ $\alpha$ ]<sub>D</sub><sup>25</sup> –45 (c 0.14 g/100 mL, MeOH); UV  $\lambda_{\max}$  (MeOH) (log  $\epsilon$ ) 205 (4.6), 226 (4.1), 330 (4.1) nm; ECD (MeOH, c 0.32 mM, 0.1 cm);  $\Delta\epsilon$  +10.8 (203 nm), –4.6 (227 nm), –1.7 (248 nm), –1.1 (332 nm); <sup>1</sup>H and <sup>13</sup>C NMR, see Table 3; HRESIMS  $m/z$  493.1669 [M + Na]<sup>+</sup> (calcd for C<sub>22</sub>H<sub>30</sub>O<sub>11</sub>Na<sup>+</sup>, 493.1680).

**Compounds 9a and 9b**. <sup>1</sup>H and <sup>13</sup>C NMR, see Table S6, Supporting Information.

(2′R)-Toddalolactone 3′-O- $\beta$ -D-glycopyranoside (**10**): yellow solid; [ $\alpha$ ]<sub>D</sub><sup>25</sup> –2.5 (c 0.12 g/100 mL, MeOH); UV  $\lambda_{\max}$  (MeOH) (log  $\epsilon$ ) 205 (4.6), 225 (4.2), 328 (4.0) nm; ECD (MeOH, c 0.21 mM, 0.1 cm);  $\Delta\epsilon$  –2.2 (202 nm), +2.6 (226 nm), +1.0 (251 nm), +0.9 (334 nm); <sup>1</sup>H and <sup>13</sup>C NMR, see Table 3; HRESIMS  $m/z$  493.1670 [M + Na]<sup>+</sup> (calcd for C<sub>22</sub>H<sub>30</sub>O<sub>11</sub>Na<sup>+</sup>, 493.1680).

(2′S)-Toddalolactone 2′-O- $\beta$ -D-glycopyranoside (**11**): yellow solid; [ $\alpha$ ]<sub>D</sub><sup>25</sup> –46 (c 0.08 g/100 mL, MeOH); UV  $\lambda_{\max}$  (MeOH) (log  $\epsilon$ ) 204 (4.5), 224 (4.1), 329 (3.9) nm; ECD (MeOH, c 0.32 mM, 0.1 cm);  $\Delta\epsilon$  +12.9 (204 nm), –5.2 (227 nm), –1.9 (248 nm), –1.5 (332 nm); <sup>1</sup>H and <sup>13</sup>C NMR, see Table 3; HRESIMS  $m/z$  493.1672 [M + Na]<sup>+</sup> (calcd for C<sub>22</sub>H<sub>30</sub>O<sub>11</sub>Na, 493.1680).

**Hazaleanin B (12)**: yellow solid; [ $\alpha$ ]<sub>D</sub><sup>25</sup> +14 (c 0.09 g/100 mL, MeOH); UV  $\lambda_{\max}$  (MeOH) (log  $\epsilon$ ) 205 (5.0), 328 (4.3) nm; ECD (MeOH, c 0.13 mM, 0.1 cm);  $\Delta\epsilon$  +43.7 (203 nm), –18.5 (218 nm), +14.5 (244 nm), +4.3 (272 nm), –1.9 (287 nm); <sup>1</sup>H and <sup>13</sup>C NMR, see Table S7, Supporting Information; HRESIMS  $m/z$  811.2758 [M + Na]<sup>+</sup> (calcd for C<sub>39</sub>H<sub>48</sub>O<sub>17</sub>Na, 811.2784).

**Hazaleanin A (13)**: white solid; [ $\alpha$ ]<sub>D</sub><sup>25</sup> –9 (c 0.05 g/100 mL, MeOH); UV  $\lambda_{\max}$  (MeOH) (log  $\epsilon$ ) 205 (4.9), 329 (4.2) nm; ECD (MeOH, c 0.13 mM, 0.1 cm);  $\Delta\epsilon$  +20.5 (208 nm), –7.3 (217 nm), +1.4 (239 nm); <sup>1</sup>H and <sup>13</sup>C NMR, see Table S7, Supporting Information; HRESIMS  $m/z$  813.2916 [M + Na]<sup>+</sup> (calcd for C<sub>39</sub>H<sub>50</sub>O<sub>17</sub>Na, 813.2940).

**N-p-Coumaroyltyramine (14)**: yellowish solid; <sup>1</sup>H and <sup>13</sup>C NMR, see Table S8, Supporting Information; HRESIMS  $m/z$  284.1274 [M + H]<sup>+</sup> (calcd for C<sub>17</sub>H<sub>18</sub>NO<sub>3</sub>, 284.1281).

**Toddalolactone (15)**: white solid; [ $\alpha$ ]<sub>D</sub><sup>25</sup> –10 (c 0.07 g/100 mL, MeOH); UV  $\lambda_{\max}$  (MeOH) (log  $\epsilon$ ) 205 (4.5), 225 (4.1), 330 (4.0) nm; ECD (MeOH, c 0.21 mM, 0.1 cm);  $\Delta\epsilon$  +3.1 (203 nm), –1.0 (229 nm); <sup>1</sup>H and <sup>13</sup>C NMR, see Table S9, Supporting Information; HRESIMS  $m/z$  309.1329 [M + Na]<sup>+</sup> (calcd for C<sub>16</sub>H<sub>20</sub>O<sub>6</sub>Na, 309.1333).

(2′S)-Toddalolactone (**15a**): colorless solid; [ $\alpha$ ]<sub>D</sub><sup>25</sup> –51 (c 0.04 g/100 mL, MeOH); UV  $\lambda_{\max}$  (MeOH) (log  $\epsilon$ ) 196 (4.8), 205 (4.7), 226 (4.4), 330 (4.1) nm; ECD (MeOH, c 0.21 mM, 0.1 cm);  $\Delta\epsilon$  +8.8 (203 nm), –6.3 (229 nm), –1.8 (256 nm), –1.7 (327 nm).

(2′R)-Toddalolactone (**15b**): colorless solid; [ $\alpha$ ]<sub>D</sub><sup>25</sup> 50 (c 0.06 g/100 mL, MeOH); UV  $\lambda_{\max}$  (MeOH) (log  $\epsilon$ ) 197 (4.7), 205 (4.6), 225 (4.3), 330 (4.0) nm; ECD (MeOH, c 0.21 mM, 0.1 cm);  $\Delta\epsilon$  +5.8 (225 nm), +2.7 (253 nm), +1.0 (329 nm).

**Ion Exchange.** The resin (Lewatit MonoPlus SP 112 (Na<sup>+</sup> form), 500 mg) was placed in a 3 mL glass vial with a magnetic stirrer. The resin was washed twice with 10 mL of HPLC grade MeOH while slowly stirring. Compound **2** or **4**, respectively, was dissolved in MeOH at a concentration of 1.7 mg/mL, added to the washed resin, and stirred until the color of the supernatant had faded. The supernatant was discarded, and the resin was washed twice with 10 mL of MeOH. Then, 1 mL of a 10% NaCl solution in H<sub>2</sub>O/MeOH (1:1) was added while stirring, followed by 5 mL of MeOH. The supernatant was collected, and the step was repeated once again. The combined supernatants were dried under a flow of N<sub>2</sub>, suspended in 1.5 mL of HPLC grade water, and centrifuged at 13 200 rpm for 8 min. The supernatant was discarded, and the precipitate was washed twice more with 1 mL of H<sub>2</sub>O, yielding the respective chloride.

**Preparation of 6a.** Compound **6** (0.1 mg, 0.4  $\mu$ mol) was dissolved in 75  $\mu$ L of DCM and 25  $\mu$ L of MeOH in a vial under an argon atmosphere, and 5  $\mu$ L of trimethylsilyl diazomethane (0.6 M in *n*-hexane, 3  $\mu$ mol) was added. The mixture was vortexed and allowed to stand at room temperature for 1 h. The reaction was stopped by the addition of 3.4  $\mu$ L of 1.7 M acetic acid in H<sub>2</sub>O. The reaction mixture was dried in a flow of N<sub>2</sub> to yield **6a**.

**Enantiomeric Excess Determination of Toddalolactone (15).** Eu(hfc)<sub>3</sub> (0.7 mg) was dissolved under argon in CDCl<sub>3</sub> at a concentration of 1.5 equiv of **15** per 120  $\mu$ L, and the solution was transferred under argon to the mixture of **15a** and **15b**. The resulting solution was transferred into a 3 mm NMR tube under argon, and <sup>1</sup>H NMR spectra were recorded.

**Acid Hydrolysis of 9, 10, and 11.** Analogous to acid hydrolysis for GCMS sugar analysis,<sup>24</sup> approximately 1 mg of **9**, **10**, or **11**, respectively, was dissolved in 1 mL of 2 N aqueous HCl in a 4 mL sealable vial. The vial was placed in an oven at 105 °C for 105 min. After cooling, the mixture was extracted with EtOAc (3  $\times$  1 mL). The organic layers were combined and dried under N<sub>2</sub>. The glycones **15a** and **15b**, respectively, were identified as minor compounds via chiral-phase HPLC on a Daicel Chiralpak IG column eluting with 20% CH<sub>3</sub>CN. (2′R)-Toddalolactone (**15b**) eluted at 4.74 min, and (2′S)-toddalolactone (**15a**) at 4.93 min, respectively (Figure S128, Supporting Information). The major compounds recovered after hydrolysis of **9**, **10**, and **11**, respectively, were the ketone **9a** and the aldehyde **9b** (Figure S18, Supporting Information).

**Enzymatic Hydrolysis of 9, 10, and 11.** Approximately 1 mg of **9**, **10**, or **11** was dissolved in 100  $\mu\text{L}$  of cellulase blend (Sigma-Aldrich, Cellulase, enzyme blend, SAE0020) diluted 1:1 with purified water. The mixture was stirred at 37  $^{\circ}\text{C}$  for 22.5 h. Afterward, the reaction mixture was diluted with 900  $\mu\text{L}$  of  $\text{H}_2\text{O}$  and extracted with  $\text{EtOAc}$  ( $3 \times 1 \text{ mL}$ ). The organic layers were combined and dried under  $\text{N}_2$ . Compounds **9** and **10** afforded their respective aglycone, while **11** was recovered unreacted.

**Computational Methods.** Conformational analysis was performed with Schrödinger MacroModel 11.0 (Schrödinger, LLC, New York) employing the OPLS2005 (optimized potential for liquid simulations) force field in  $\text{H}_2\text{O}$  for geometrical optimization in two steps. In the first step, a global minimum was searched using 20 000 or 30 000 steps, depending on the size of the molecule. In the second step, the global minimum was used for a conformational search (4000 steps) choosing the five conformers to be subjected to geometrical optimization and energy calculation applying DFT with Becke's nonlocal three-parameter exchange and correlation functional and the Lee–Yang–Parr correlation functional level (B3LYP), using the B3LYP/6-31G\*\* basis set, the SCRF method, and the CPMC model for solvation (MeOH for ECD calculations) with the Gaussian 09 program package.<sup>39</sup> Excitation energy (denoted by wavelength in nm), rotator strength ( $R_{\text{str}}$ ), dipole velocity ( $R_{\text{vel}}$ ), and dipole length ( $R_{\text{len}}$ ) were calculated in MeOH by TD-DFT/B3LYP/6-31G(d,p). ECD curves were obtained on the basis of rotator strengths with a half-band of 0.25 eV using SpecDis v1.71.<sup>40</sup>

**Conformational Search for 13.** The conformational flexibility and relative structural complexity of **13** required a more sophisticated conformational analysis. The 3D structures of all four stereoisomers were built in the Maestro modeling environment.<sup>41</sup> First, a conformational search was performed to obtain a reasonable starting conformation by sampling a total of 30 000 conformers using a mixed torsional/low-mode sampling method, extended torsional sampling, OPLS 2005 force field, and the implicit water solvent model in MacroModel.<sup>42</sup> The water solvent model was selected from the list of available implicit models (water,  $\text{CHCl}_3$ , octanol), because it offers properties closest to MeOH. Next, a periodic boundary system was created by placing the global minimum structure identified in the conformational search into a cubic system (edge length 50 Å) of preorganized MeOH molecules. The whole periodic boundary system was fully optimized using the default relaxation protocol implemented in Desmond,<sup>43–45</sup> composed of seven stages allowing the solvent molecules to optimally arrange with respect to the solute. The last frame of the equilibration stage was used as input for the production simulation in the total duration of 0.48 ms (NPT ensemble and standard conditions  $T = 300 \text{ K}$ ,  $p = 101.325 \text{ kPa}$ ) with frames being sampled every 480 ps (in total 1000 frames were saved per simulation). All MD simulations were done using Desmond software. The MD trajectories were postprocessed using the default clustering analysis of Desmond. Representative solute structures of the 10 most significant clusters were used as input for Gaussian 09 calculations as described earlier.

**Ethics Statement.** Patients gave their written consent to donate blood for scientific research. All experiments conducted on human material were approved by the Ethics Committee of the University of Freiburg (55/14; 11.02.2014), and all methods used were compliant with the regulations of the Ethics Committee.

**Preparation and Cultivation of Human Peripheral Lymphocytes.** Peripheral blood mononuclear cells (PBMCs) were isolated from the blood of healthy adult donors obtained from the Blood Transfusion Centre (University Medical Center, Freiburg, Germany). Venous blood was centrifuged on a LymphoPrep gradient (density: 1.077  $\text{g}/\text{cm}^3$ , 20 min, 500g, 20  $^{\circ}\text{C}$ ; Progen). After centrifugation, cells were washed twice with PBS and subsequently cultured in RPMI 1640 medium supplemented with 10% heat-inactivated fetal calf serum (GE Healthcare Life Sciences), 2 mM L-glutamine, 100 U/mL penicillin, and 100 U/mL streptomycin (all from Life Technologies). The cells were cultured at 37  $^{\circ}\text{C}$  in a humidified incubator with a 5%  $\text{CO}_2$ /95% air atmosphere.

**T Cell Proliferation Assay.** Lymphocytes were isolated, washed twice in cold PBS, and resuspended in PBS at a concentration of  $5 \times 10^6$  cells/mL. Cells were stained for 10 min at 37  $^{\circ}\text{C}$  with carboxyfluorescein diacetate succinimidyl ester (CFSE; 5  $\mu\text{M}$ ; Sigma-Aldrich, St. Louis, MO, USA). The staining was stopped by washing twice with complete medium. Stained lymphocytes ( $2 \times 10^6$  cells/mL) were stimulated with anti-human CD3 (clone OKT3) and anti-human CD28 (clone 28.2) mAbs (each 100 ng/mL; eBioscience) in the presence of either medium, CsA (4.16  $\mu\text{M}$ ; Novartis Pharma), CPT (300  $\mu\text{M}$ ; Tocris), or plant extracts/single compounds (concentration range 0.3–30  $\mu\text{M}$ ) and incubated for 72 h. The negative control remained unstimulated. Flow cytometric analysis of the cell division was performed using a FACSCalibur instrument (BD Biosciences).

**Determination of Apoptosis and Necrosis of T Cells.** Lymphocytes were isolated, washed twice in cold PBS, and resuspended in medium at a concentration of  $2 \times 10^6$  cells/mL. Cells were stimulated with anti-human CD3 (clone OKT3) and anti-human CD28 (clone 28.2) mAbs (each 100 ng/mL; eBioscience) in the presence of either medium, CPT (300  $\mu\text{M}$ ; Tocris), 0.5% Triton-X 100, or plant extracts and cultivated for 48 h. The negative control remained unstimulated. Cultured cells were washed with PBS and stained with annexin V-FITC using the apoptosis detection kit (eBioscience) according to the manufacturer's instructions. Propidium iodide (eBioscience) was added and cells were stained for 15 min at room temperature in the dark. Apoptosis and necrosis rates were determined by flow cytometric analysis using a FACSCalibur instrument (BD Biosciences).

**Testing of Microfractions.** The dried microfractions in 96-deep-well plates were dissolved in 25  $\mu\text{L}$  of DMSO by sonication and mixing with a pipet. Of these stock solutions, dilutions of 1/1, 1/3, 1/10, and 1/30 were prepared and tested in duplicates for T lymphocyte proliferation inhibition as described above. Assuming an equal distribution of 200 ng substance in each of the microfractions, theoretical  $\text{IC}_{50}$  values were calculated as a relative measure of activity. They were normalized to 100%, with the highest value representing 100%.

**Analysis of Data.** For statistical analysis, data were processed with Microsoft Excel and SPSS software (IBM, version 22.0, Armonk, USA). Statistical significance was determined with the SPSS software. Statistical significance was determined with the SPSS software by a one-way ANOVA, followed by Dunnett's post hoc pairwise comparisons. Values are presented as mean  $\pm$  SD for the indicated number of independent experiments. The asterisks represent significant differences from controls ( $*p < 0.05$ ).

## ■ ASSOCIATED CONTENT

### Supporting Information

The Supporting Information is available free of charge at <https://pubs.acs.org/doi/10.1021/acs.jnatprod.0c00564>.

T lymphocyte proliferation data for *T. asiatica* MeOH extract,  $^1\text{H}$  and  $^{13}\text{C}$  NMR data for compounds **1–5**, **6a**, **8**, and **12–15**; experimental and computed ECD spectra of **7**, **8**, **11**, and **15** as well as UV spectra for compounds **7–13** and **15**; 1D and 2D NMR spectra and chiral-phase HPLC data (PDF)

## ■ AUTHOR INFORMATION

### Corresponding Author

Matthias Hamburger – Pharmaceutical Biology, Pharmazentrum, University of Basel, 4056 Basel, Switzerland; [orcid.org/0000-0001-9331-273X](https://orcid.org/0000-0001-9331-273X); Phone: +41 61 207 14 25; Email: [matthias.hamburger@unibas.ch](mailto:matthias.hamburger@unibas.ch); Fax: +41 61 207 14 74

## Authors

**Jakob K. Reinhardt** – Pharmaceutical Biology, Pharmacenter, University of Basel, 4056 Basel, Switzerland

**Amy M. Zimmermann-Klemd** – Center for Complementary Medicine, Institute for Infection Prevention and Hospital Epidemiology, Faculty of Medicine, University of Freiburg, 79106 Freiburg, Germany

**Ombeline Danton** – Pharmaceutical Biology, Pharmacenter, University of Basel, 4056 Basel, Switzerland

**Martin Smieško** – Pharmacenter, University of Basel, 4056 Basel, Switzerland; [orcid.org/0000-0003-2758-2680](https://orcid.org/0000-0003-2758-2680)

**Carsten Gründemann** – Pharmacenter, University of Basel, 4056 Basel, Switzerland

Complete contact information is available at:

<https://pubs.acs.org/10.1021/acs.jnatprod.0c00564>

## Notes

The authors declare no competing financial interest.

## ACKNOWLEDGMENTS

C.G. is supported by PRIAM-BS (Verein Stiftungsprofessur für Integrative and Anthroposophische Medizin an der Universität Basel). ECD spectra were measured at the Biophysics Facility, Biozentrum, University of Basel. We are grateful to Andrea Treyer for measuring the HRESIMS data and to Orlando Fertig for technical support. Assunta Green, Daicel Technologies Europe, is gratefully acknowledged for providing the chiral-phase HPLC columns.

## REFERENCES

- (1) Davidson, A.; Diamond, B. *N. Engl. J. Med.* **2001**, *345* (5), 340–350.
- (2) Skapenko, A.; Leipe, J.; Lipsky, P. E.; Schulze-Koops, H. *Arthritis Res. Ther.* **2005**, *7*, S4–S14.
- (3) Her, M.; Kavanaugh, A. *J. Allergy Clin. Immunol.* **2016**, *137* (1), 19–27.
- (4) *Toddalia asiatica*; US National Plant Germplasm System. <https://npgsweb.ars-grin.gov/gringlobal/taxonomydetail.aspx?36738> (24.04.2020).
- (5) Zhou, J.; Xie, G.; Yan, X. *Isolated Compounds (T-Z) References TCM Plants and Congeners*; Springer: Berlin, Heidelberg, 2011; Vol. 5, p 455.
- (6) Orwa, J. A.; Jondiko, I. J. O.; Minja, R. J. A.; Bekunda, M. J. *Ethnopharmacol.* **2008**, *115*, 257–262.
- (7) Rajkumar, M.; Chandra, R. H.; Asres, K.; Veeresham, C. *Pharmacogn. Rev.* **2008**, *2* (4), 386–397.
- (8) Li, W.; Zhang, J.-S.; Huang, J.-L.; Jiang, M.-H.; Xu, Y.-K.; Ahmed, A.; Yin, S.; Tang, G.-H. *RSC Adv.* **2017**, *7*, 31061–31068.
- (9) Hu, J.; Shi, X.; Chen, J.; Mao, X.; Zhu, L.; Yu, L.; Shi, J. *Food Chem.* **2014**, *148*, 437–444.
- (10) Hirunwong, C.; Sukieum, S.; Phatchana, R.; Yenjai, C. *Phytochem. Lett.* **2016**, *17*, 242–246.
- (11) Potterat, O.; Hamburger, M. *Nat. Prod. Rep.* **2013**, *30*, S46–64.
- (12) Tian, X.; Guo, S.; He, K.; Roller, M.; Yang, M.; Liu, Q.; Zhang, L.; Ho, C.-T.; Bai, N. *Nat. Prod. Res.* **2018**, *32* (3), 354–357.
- (13) Takahashi, H.; Iguchi, M.; Onda, M. *Chem. Pharm. Bull.* **1985**, *33* (11), 4775–4782.
- (14) Nakanishi, T.; Suzuki, M. *J. Nat. Prod.* **1998**, *61*, 1263–1267.
- (15) Ishii, H.; Ishikawa, T.; Ichikawa, Y.; Sakamoto, M.; Ishikawa, M.; Takahashi, T. *Chem. Pharm. Bull.* **1984**, *32* (8), 2984–2994.
- (16) Bunting, J. W. Heterocyclic Pseudobases. In *Advances in Heterocyclic Chemistry*; Katritzky, A. R.; Boulton, A. J., Eds.; Academic Press, 1980; Vol. 25, pp 1–82.
- (17) Ramani, P.; Fontana, G. *Tetrahedron Lett.* **2008**, *49*, 5262–5264.
- (18) Schramm, A.; Hamburger, M. *Fitoterapia* **2014**, *94*, 127–33.
- (19) Lv, P.; Huang, K.; Xie, L.; Xu, X. *Org. Biomol. Chem.* **2011**, *9*, 3133–5.
- (20) De, S.; Mishra, S.; Kakde, B. N.; Dey, D.; Bisai, A. *J. Org. Chem.* **2013**, *78*, 7823–7844.
- (21) Arthur, H. R.; Ng, Y. L. *J. Chem. Soc.* **1959**, 4010–4012.
- (22) Huang, S.-C.; Chen, M.-T.; Wu, T.-S. *Phytochemistry* **1989**, *28* (12), 3574–3576.
- (23) Okamura, N.; Haraguchi, H.; Hashimoto, K.; Yagi, A. *Phytochemistry* **1994**, *37* (5), 1463–1466.
- (24) Severi, J. A.; Fertig, O.; Plitzko, I.; Vilegas, W.; Hamburger, M.; Potterat, O. *Helv. Chim. Acta* **2010**, *93*, 1058–1066.
- (25) Lin, T. T.; Huang, Y. Y.; Tang, G. H.; Cheng, Z. B.; Liu, X.; Luo, H. B.; Yin, S. *J. Nat. Prod.* **2014**, *77*, 955–62.
- (26) Li, Y.; Sun, S.-W.; Zhang, X.-Y.; Liu, Y.; Liu, X.-H.; Zhang, S.; Wang, W.; Wang, J.; Wang, W. *Plants* **2020**, *9* (4), 428.
- (27) Shibuya, H.; Takeda, Y.; Zhang, R.-s.; Tanitame, A.; Tsai, Y.-L.; Kitagawa, I. *Chem. Pharm. Bull.* **1992**, *40* (10), 2639–2346.
- (28) Gao, H.-y.; Wang, H.-y.; Li, G.-y.; Du, X.-w.; Zhang, X.-t.; Han, Y.; Huang, J.; Li, X.-x.; Wang, J.-h. *Phytochem. Lett.* **2014**, *7*, 150–155.
- (29) Chang, Y.-C.; Chen, C.-Y.; Chang, F.-R.; Wu, Y.-C. *J. Chin. Chem. Soc.* **2001**, *48*, 811–815.
- (30) Sharma, P. N.; Shoeb, A.; Kapil, R. S.; Popli, S. P. *Phytochemistry* **1981**, *20*, 335–336.
- (31) Ishii, H.; Kobayashi, J.-I.; Sakurada, E.; Ishikawa, T. *J. Chem. Soc., Perkin Trans. 1* **1992**, *1* (13), 1681–1684.
- (32) Ishii, H.; Kobayashi, J.; Ishikawa, M.; Haginiwa, J.; Ishikawa, T. *Yakugaku Zasshi* **1991**, *111* (7), 365–375.
- (33) El-Khatib, R. M.; Nassr, L. A.-M. E. *Spectrochim. Acta, Part A* **2007**, *67*, 643–648.
- (34) Rao, G. K.; Gowda, N. B.; Ramakrishna, R. A. *Synth. Commun.* **2012**, *42*, 893–904.
- (35) Yuan, Y.; Zhu, F.; Pu, Y.; Wang, D.; Huang, A.; Hu, X.; Qin, S.; Sun, X.; Su, Z.; He, C. *Brain, Behav., Immun.* **2015**, *48*, 287–300.
- (36) Zhai, H.; Hu, S.; Liu, T.; Wang, F.; Wang, X.; Wu, G.; Zhang, Y.; Sui, M.; Liu, H.; Jiang, L. *Mol. Med. Rep.* **2016**, *13*, 2536–2542.
- (37) Li, J.; Su, J.; Shan, L.; Zhang, S.; Zhang, W.; Dai, X.; Cao, X.; Yu, Y. Patent CN102008474B, 2010.
- (38) Iwasaki, H.; Oku, H.; Takara, R.; Miyahira, H.; Hanashiro, K.; Yoshida, Y.; Kamada, Y.; Toyokawa, T.; Takara, K.; Inafuku, M. *Cancer Chemother. Pharmacol.* **2006**, *58*, 451–459.
- (39) Frisch, M. J.; Trucks, G. W.; Schlegel, H. B.; Scuseria, G. E.; Robb, M. A.; Cheeseman, J. R.; Scalmani, G.; Barone, V.; Mennucci, B.; Petersson, G. A.; Nakatsuji, H.; Caricato, M.; Li, X. H. H. P.; Izmaylov, A. F.; Bloino, J. Z. G.; Sonnenberg, J. L.; Hada, M.; Ehara, M.; Toyota, K.; Fukuda, R.; Hasegawa, J.; Ishida, M.; Nakajima, T.; Honda, Y.; Kitao, O.; Nakai, H.; Vreven, T.; Montgomery, J. A., Jr.; Peralta, J. E.; Ogliaro, F.; Bearpark, M. J.; Heyd, J.; Brothers, E. N.; Kudin, K. N.; Staroverov, V. N.; Kobayashi, R.; Normand, J.; Raghavachari, K.; Rendell, A. P.; Burant, J. C.; Iyengar, S. S.; Tomasi, J.; Cossi, M.; Rega, N.; Millam, N. J.; Klene, M.; Knox, J. E.; Cross, J. B.; Bakken, V.; Adamo, C.; Jaramillo, J.; Gomperts, R.; Stratmann, R. E.; Yazyev, O.; Austin, A. J.; Cammi, R.; Pomelli, C.; Ochterski, J. W.; Martin, R. L.; Morokuma, K.; Zakrzewski, V. G.; Voth, G. A.; Salvador, P.; Dannenberg, J. J.; Dapprich, S.; Daniels, A. D.; Farkas, O.; Foresman, J. B.; Ortiz, J. V.; Cioslowski, J.; Fox, D. J. *Gaussian 09*; Gaussian, Inc.: Wallingford, CT, USA, 2009.
- (40) Bruhn, T.; Schaumlöffel, A.; Hemberger, Y. *Spec Dis*, 1.64; University of Würzburg: Germany, 2015.
- (41) *Maestro*, 11.0; Schrödinger, LLC: New York, NY, 2016.
- (42) *Macro Model*, 11.0; Schrödinger, LLC: New York, NY, 2016.
- (43) *Desmond Molecular Dynamics System*, 5.7; D. E. Shaw Research: New York, NY, 2019.
- (44) *Desmond Interoperability Tools*, 11.0; Schrödinger, LLC: New York, NY, 2019.
- (45) Bowers, K. J.; Chow, E.; Xu, H.; Dror, R. O.; Eastwood, M. P.; Gregersen, B. A.; Klepeis, J. L.; Kolossvary, I.; Moraes, M. A.; Sacerdoti, F. D.; Salmon, J. K.; Shan, Y.; Shaw, D. E. *Proceedings of the 2006 ACM/IEEE Conference on Supercomputing*; Association for Computing Machinery: Tampa, FL, 2006; pp 84-es.